Highlight Review

Structures and Sorption Properties of Ionic Crystals of Polyoxometalates with Macrocation

Noritaka Mizuno* and Sayaka Uchida

(Received February 15, 2006; CL-068003)

Abstract

Polyoxometalates are nanosized metal–oxygen macroanions and suitable building blocks of ionic crystals with nanostructures in combination with appropriate macrocations. In this review, (1) formation of ionic crystals by the complexation of the polyoxometalates with a macrocation and the hydrophilic guest sorption properties, (2) effects of charges of polyoxometalates on the structures and sorption properties of ionic crystals, and (3) construction of both hydrophilic and hydrophobic channels in the crystal lattice of the polyoxometalate based ionic crystals are highlighted.

♦ Introduction

Extensive researches have been devoted to the syntheses of nanostructured materials, which show the unique selectivity in the guest sorption, ion exchange, and catalysis. As shown in Figure 1, nanostructured materials can be classified into three groups by the kinds of chemical bonds to construct the framework; (i) inorganic zeolites (covalent bonds), (ii) metal–organic frameworks (organic zeolites) (coordination bonds), and (iii) layered compounds and ionic crystals (hydrogen bonds and/or ionic bonds).

Inorganic zeolites are composed of covalently bonded [TO_4] (T = Si, Al, P, etc.) and [MO_6] (M = Ti, Zr, Sn, etc.) units and contain well-ordered nanosized pores (ca. 3–15 Å).[1–3] Inorganic zeolites show the molecular sieving effects depending on the framework geometry and pore size. A classical example is a Ca–A zeolite, which possesses eight-membered ring and pore size of 5 Å and adsorbs straight-chain organic molecules but not those that are branched.[4] As for the separation of inorganic gases, the titanosilicate of which the effective pore size can be finely tuned by the dehydration at elevated temperatures can separate 3–4 Å molecules such as N_2/CH_4, Ar/O_2, and N_2/O_2, with the pressure-swing adsorption.[3]

Recently, much attention has been paid toward the syntheses of porous metal–organic frameworks constructed with the coordination bonds between the metal and organic building units.[5–14] The framework geometry and pore size of these compounds can be finely tuned by the choice of building blocks. For example, a kind of metal–organic framework with zinc–benzenecarboxylate, IRMOF-16, shows the highest free volume (91.1%) and the lowest density (0.21 g cm^{-3}) among those reported for crystalline materials.[12] As for the separation of inorganic gases with the metal–organic frameworks, porous manganese formate[13] and lanthanide carboxylate[14] sorb carbon dioxide but not argon and dinitrogen (kinetic diameters: CO_2 = 3.30 Å, Ar = 3.40 Å, and N_2 = 3.64 Å), showing combined effects of pore sizes and host–guest interactions. Although various kinds of zeolites and metal–organic frameworks can sorb small organic molecules, the discrimination of small organic molecules (especially ≤ C3) and/or close-boiling mixtures are still rare.[15–20]

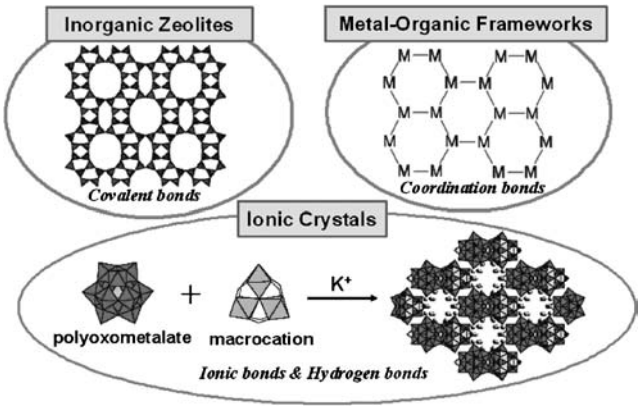

Figure 1. Classification of nano-structured materials.

Layered compounds such as montmorillonites and mixed-metal layered hydroxides possess cations or anions in the interlayer space, and the layered structures are stabilized by the ionic bonds and hydrogen bonds.[21,22] The layered compounds swell in water and polar organic solvents with the expansion of the interlayer space.[23–26] Recently, the control of the morphology and porosity of ionic crystals such as metal carbonates and sulfates has been extensively studied.[27] Since ionic bonds are formed by the strong Coulomb interactions between anions and cations, the bonds are isotropic and the ions are often densely packed in the crystal lattice. Therefore, pores exist mainly between the primary particles of ionic crystals, and the extent of porosity is controlled empirically by changing the degree of supersaturation of the synthetic solution.[28–30]

Polyoxometalates are nanosized metal–oxygen macroanions and suitable building blocks of ionic crystals with nano-structures in combination with appropriate macrocations.[31–41] Polyoxometalates show unique redox or acidic properties, which

Prof. Noritaka Mizuno, Dr. Sayaka Uchida*
Department of Applied Chemistry, School of Engineering, The University of Tokyo,
7-3-1 Hongo, Bunkyo-ku, Tokyo 113-8656
Core Research for Evolutional Science and Technology (CREST), Japan Science and Technology Agency,
4-1-8 Honcho, Kawaguchi 332-0012
E-mail: tmizuno@mail.ecc.u-tokyo.ac.jp

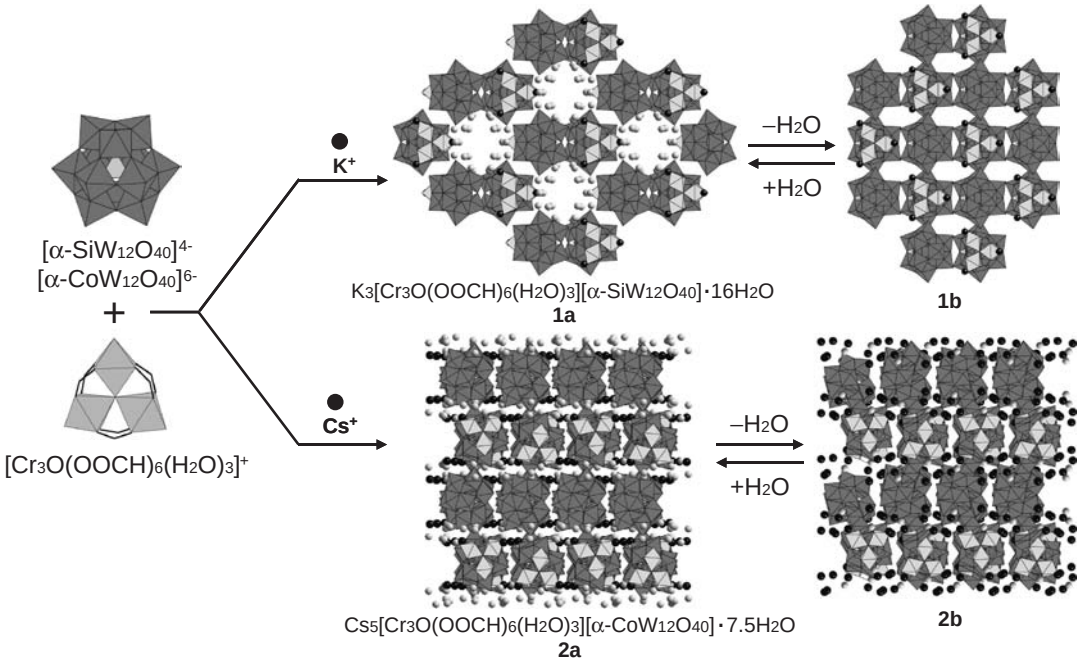

Figure 2. Crystal structures of **1a**/**1b** and **2a**/**2b**. Dark gray and light gray polyhedra in the polyoxometalates are $[WO_6]$ and $[XO_4]$ (X = Si and Co) units, respectively. Light gray polyhedra in the macrocation are $[CrO_6]$ units. Black and white spheres are alkali metal atoms (K^+ or Cs^+) and oxygen atom of the water of crystallization, respectively.

can be controlled at atomic or molecular levels and have been applied to catalysis.[42–49]

Recently, we have reported that the complexation of Keggin-type polyoxometalates of $[\alpha\text{-}SiW_{12}O_{40}]^{4-}$ and $[\alpha\text{-}CoW_{12}O_{40}]^{6-}$ with a macrocation of $[Cr_3O(OOCH)_6(H_2O)_3]^+$ forms ionic crystals of $K_3[Cr_3O(OOCH)_6(H_2O)_3][\alpha\text{-}SiW_{12}O_{40}]\cdot 16H_2O$[50,51] and $Cs_5[Cr_3O(OOCH)_6(H_2O)_3][\alpha\text{-}CoW_{12}O_{40}]\cdot 7.5H_2O$,[52] respectively. The ionic crystals possess hydrophilic channels filled with the water of crystallization. The water of crystallization was desorbed by the evacuation at room temperature to form a guest free phase. The former guest free phase sorbs polar organic molecules up to C2,[50,51] while the latter guest free phase sorbs only water.[52] In addition, it is demonstrated that the void sizes of ionic crystals of Dawson-type polyoxometalates ($[\alpha\text{-}P_2V_xW_{18-x}O_{62}]^{m-}$) with the macrocation increase with the decrease in m and can be controlled.[53] While the use of a macrocation of $[Cr_3O(OOCH)_6(H_2O)_3]^+$ formed only hydrophilic channels, the use of a macrocation of $[Cr_3O(OOCC_2H_5)_6(H_2O)_3]^+$ formed both hydrophobic and hydrophilic channels in the crystal lattice.[54] In this review, our recent works on (1) the formation of ionic crystals by the complexation of polyoxometalates with the large macrocation and the hydrophilic guest sorption properties, (2) the effects of charges of polyoxometalates on the structures and sorption properties of ionic crystals, and (3) the construction of both hydrophilic and hydrophobic channels in the crystal lattice of the polyoxometalate-based ionic crystals are highlighted.

♦ *Formation of Ionic Crystals of Polyoxometalates with Macrocation*

Figure 2 shows the schematic syntheses and crystal structures of $K_3[Cr_3O(OOCH)_6(H_2O)_3][\alpha\text{-}SiW_{12}O_{40}]\cdot 16H_2O$ [**1a**] and $Cs_5[Cr_3O(OOCH)_6(H_2O)_3][\alpha\text{-}CoW_{12}O_{40}]\cdot 7.5H_2O$ [**2a**]. Elemental analyses of **1a** and **2a** showed that the macrocation/polyoxometalate ratios were 1:1, and the surplus anion charge was neutralized by the alkali metal ions. The polyoxometalates and macrocations lined up alternately to form columns, which were arranged in a honeycomb (**1a**) or densely packed (**2a**). The lengths between the carbon atoms of the bridging formates in the macrocations and the oxygen atoms of the polyoxometalates in the same column were in hydrogen-bonding distances (C–H···O distances were 3.25–3.37 and 2.81–3.07 Å for **1a** and **2a**, respectively). The spaces between the columns were occupied with the water of crystallization and the space volumes for **1a** and **2a** corresponded to 36 and 17% of the crystal lattices, respectively. Thus, the space volumes of the crystal lattices increased with the decrease in n of $[\alpha\text{-}XW_{12}O_{40}]^{n-}$ (X = Si, $n = 4$; X = Co, $n = 6$). This is probably because the anion–cation interactions decrease with the decrease in n.

The water of crystallization in **1a** and **2a** was either in the vicinity of the alkali metal ion or hydrogen bonded to the constituent ions (polyoxometalate and macrocation) or to the other water molecules. The water of crystallization in **1a** was completely desorbed by the evacuation at room temperature, while about 50% of the water of crystallization in **2a** was desorbed. The respective **1a** and **2a** after the evacuation at room temperature were denoted by **1b** and **2b**, respectively. The observed XRD pattern of **1b** was fairly well reproduced by the structure **1b** showing the close packing of the columns (Figure 2). The crystal structure of **2b** was solved by the single-crystal X-ray structure analysis. The arrangements of the polyoxometalates and macrocations in **2b** were essentially the same as those in **2a**, while small reduction in the a (−0.316 Å) and b axes

Published on the web (Advance View) May 30, 2006; doi:10.1246/cl.2006.688

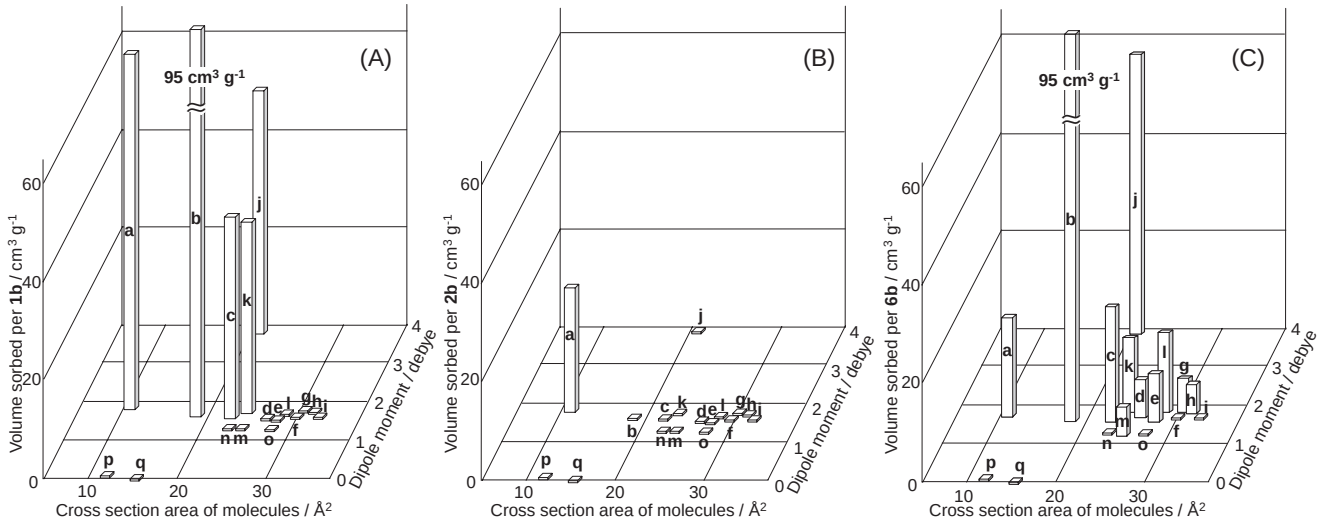

Figure 3. Effects of the cross section areas and the dipole moments of guest molecules on the sorption properties of **1b**, **2b**, and **6b** ($P/P_0 = 0.7$ at 298 K). (A) **1b**, (B) **2b**, and (C) **6b**. (a) Water, (b) methanol, (c) ethanol, (d) 1-propanol, (e) 2-propanol, (f) 1-butanol, (g) 2-butanol, (h) *iso*-butanol, (i) *tert*-butanol, (j) acetonitrile, (k) methyl formate, (l) methyl acetate, (m) dimethyl ether, (n) dichloromethane, (o) 1,2-dichloroethane, (p) nitrogen monoxide, and (q) dinitrogen.

(−0.696 Å) of the lattice was observed (Figure 2). Therefore, structures **1b** and **2b** showed the close packing of the columns. The calculated cell volumes per formula (V/Z) were in the order of **1b** (1467 Å^3) > **2b** (1406 Å^3) and decreased with the increase in n of $[\alpha\text{-}XW_{12}O_{40}]^{n-}$ (X = Co, $n = 4$; X = Si, $n = 6$). This is probably because the anion–cation interaction increased with the increase in n, and the constituent ions were more closely packed. The BET surface areas of **1b** and **2b** were small (<2 m^2 g^{-1}) in accord with the close packing of the columns where no micropores existed. The crystal structures of **1a** and **2a** were completely restored by the exposure of **1b** and **2b** to the saturated water vapor at room temperature.

Figure 3A summarizes the amounts of sorption for **1b** at P/P_0 of 0.7. The compound **1b** reversibly sorbed various kinds of polar hydrogen-bonding (hydrophilic) organic molecules such as ≤C2 alcohols, nitriles, and esters as well as water. As for ethanol, acetonirile, and methyl formate, the amounts were small at $P/P_0 = 0.4$ and increased suddenly at definite pressures (gate pressures). Neither non-hydrogen-bonding (hydrophobic) chlorocarbons nor molecules without or with small polarity such as nitrogen monoxide and dinitrogen were sorbed despite the small sizes. Thus, the guest inclusion property of **1b** seems to be affected by the molecular size and the dipole moments of the guest molecules.

Figure 3B summarizes the amounts of sorption for **2b**. The compound **2b** sorbed only water, and the sizes of the polar molecules sorbed decreased with the increase in n of $[\alpha\text{-}XW_{12}O_{40}]^{n-}$ from **1b** to **2b**. The water sorption property of **2b** was applied to the removal of water from highly pure ethanol: The compound **2b** sorbed only water and the concentration was decreased from 0.23 to 0.08 wt % at 298 K. The complex **2b** could be recycled only by the separation from the ethanol solution with decantation followed by the evacuation at room temperature. The amount of removed water remained unchanged even after six cycles and **2b** could be easily recyclable.

♦ *Effect of Charges on the Structures and Sorption Properties*

Next, the complexation of α-Dawson-type $[\alpha\text{-}P_2V_xW_{18-x}O_{62}]^{m-}$ polyoxometalates (D_{3h} symmetry) with the macrocation of $[Cr_3O(OOCH)_6(H_2O)_3]^+$ was attempted to clarify the effects of the anion charges on the crystal structures.

The crystal structure and the crystallographic data of $(NH_4)_4[Cr_3O(OOCH)_6(H_2O)_3]_2[\alpha\text{-}P_2W_{18}O_{62}]\cdot 15H_2O$ [**3a**] are shown in Figure 4 and Table 1, respectively. The structure of **3a** was well described by the two types of columns (I and II) running along the c axis. The column I was composed of polyoxometalates and macrocations which were placed alternately along the c axis. The column II contained only macrocations which were disordered between the two positions along the c axis with an occupancy of 0.5. As shown in Figure 4a, the column I assembled to form a honeycomb in the ab plane and the column II existed inside the honeycomb. Thus, the symmetry of the polyoxometalates (D_{3h}) and macrocations (D_{3h}) reflected on the crystal structure of **3a** (hexagonal, $P6_3/m$). As indicated by the broken lines in Figure 4b, multiple hydrogen bonds existed between the columns. The multiple hydrogen bonds among the constituent ions probably contribute to the stabilization of the crystal structure of **3a**.

The powder X-ray structure analyses of $(NH_4)_5[Cr_3O(OOCH)_6(H_2O)_3]_2[\alpha\text{-}P_2VW_{17}O_{62}]\cdot 15H_2O$ [**4a**] and $(NH_4)_7$-

Table 1. Lattice constants and volumes of **3a**–**5a** and **3b**–**5b**[a]

	3a	**3b**	**4a**	**4b**	**5a**	**5b**
a/Å	16.009	15.524	15.984	15.588	15.957	15.791
c/Å	21.785	20.744	21.611	20.487	20.922	18.836
V/Å^3	4835	4329	4781	4311	4613	4067

[a]Lattice constants (a, c, V) of **3a**, **4a**, and **5a** were obtained from the single-crystal X-ray analyses and those of **3b**, **4b**, and **5b** were calculated from the powder XRD patterns.

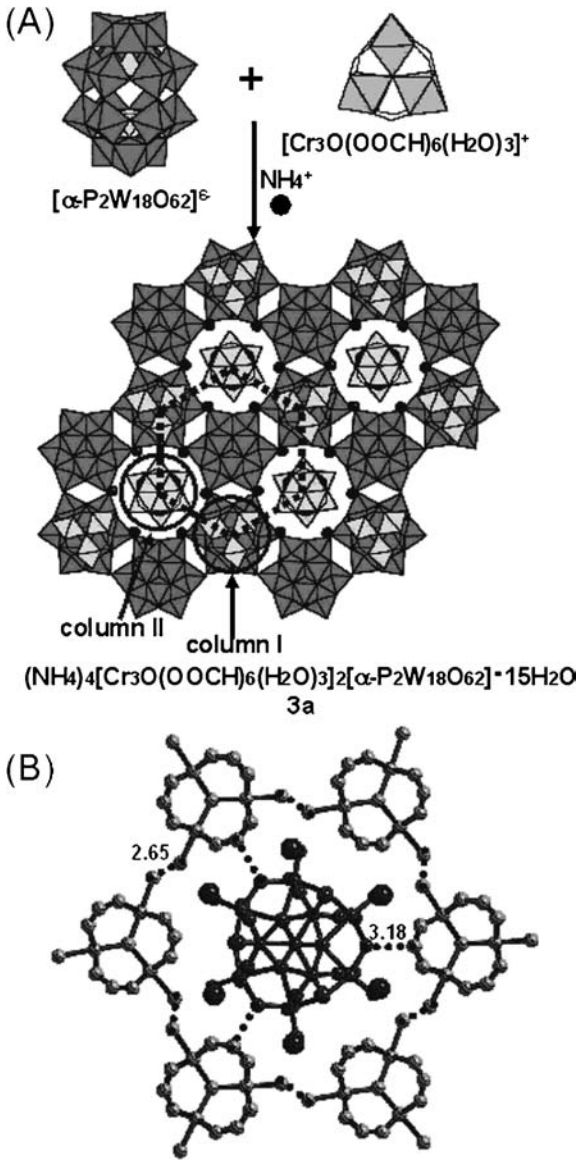

Figure 4. Crystal structure of **3a**. (A) Polyhedral and (B) ball and stick model. Dark gray and light gray polyhedra in the polyoxometalates are $[WO_6]$ and $[PO_4]$ units, respectively. Light gray polyhedra in the macrocation are $[CrO_6]$ units. Black and white spheres are ammonium ion and oxygen atom of the water of crystallization, respectively. Hydrogen bonds are shown by the dotted lines.

$[Cr_3O(OOCH)_6(H_2O)_3]_2[\alpha\text{-}P_2V_3W_{15}O_{62}]\cdot 15H_2O$ [**5a**] have shown that the crystal structures were also described by the honeycomb packing of the polyoxometalates and macrocation. Thus, in the case of ionic crystals of Dawson-type polyoxometalates, honeycomb packing of the constituent ions was realized regardless of the anion charge (−6– −9) of the polyoxometalates.

The lattice constants of **3a**–**5a** obtained from the calculations are summarized in Table 1. While the lengths of the *a* axes were almost the same among **3a**–**5a** (15.957–16.009 Å), those of the *c* axes decreased in the order of **3a** (21.785 Å) ≥ **4a** (21.611 Å) > **5a** (20.922 Å). The decrease in the *c* axes is probably due to the increase in the anion–cation interaction with increase in the anion charge.

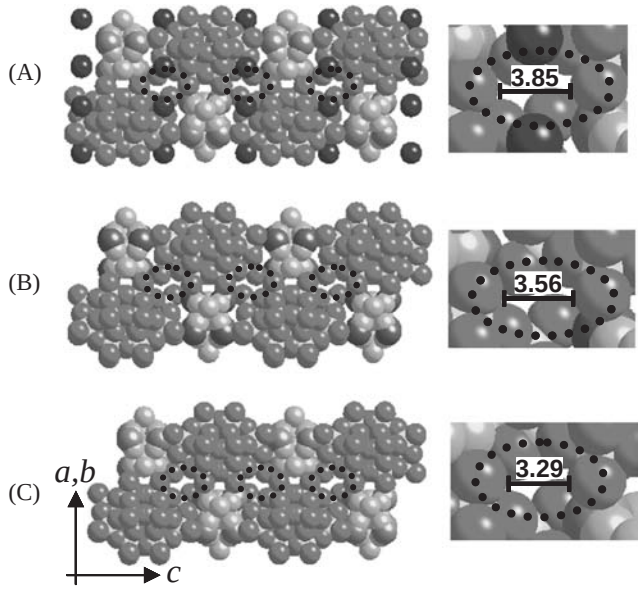

Figure 5. Space filling models showing the arrangements of the constituent ions in column I for (A) **3b**, (B) **4b**, and (C) **5b**. Dotted lines indicate the voids. The models at the right show the magnified view.

The water of crystallization in **3a**–**5a** was completely desorbed by the evacuation at 473 K, and formed the respective guest free phase **3b**–**5b**. The powder X-ray structure analyses of **3b**–**5b** showed that the experimental patterns of **3b**–**5b** were well reproduced by the calculations with structural models of the honeycomb packing. The lattice constants of **3b**–**5b** obtained from the calculation are also summarized in Table 1. While the lengths of the *a* axes were almost the same among **3b**–**5b** (15.524–15.791 Å), those of the *c* axes decreased in the order of **3b** (20.744 Å) ≥ **4b** (20.487 Å) > **5b** (18.836 Å). The decrease in the *c* axes is possibly explained by the increase in the anion–cation interaction with increase in the anion charge. Such decrease was also observed in the lengths of the *c* axes of **3a**–**5a**. Figures 5A–5C shows the space filling models of the arrangements of the constituent ions along the *c* axis in **3b**–**5b**, respectively. The compounds **3b**–**5b** possessed voids running perpendicular to the *c* axis and had no voids in the *ab* plane. In Figure 5, voids with the widest openings were indicated by the broken circles. The widest voids were created between the oxygen atoms of the polyoxometalates of the neighboring columns. The cross section diameters decreased in the order of **3b** (3.85 Å) > **4b** (3.56 Å) > **5b** (3.29 Å). The decrease in the sizes of the voids is probably due to the increase in the anion–cation interaction. The sizes of the voids are comparable to or larger than the diameter of the water molecule (3.10 Å). Thus, the sorption properties of **3b**–**5b** for small polar molecules (water, methanol, and ethanol) were investigated. While **3b** sorbed water, methanol, and ethanol from the low vapor pressures, **4b** showed gate pressures for methanol and ethanol, and **5b** could not sorb ethanol.

To summarize, the ionic crystals **3a**/**3b**, **4a**/**4b**, and **5a**/**5b** showed the honeycomb packing of the constituent ions regardless of the anion charge of the polyoxometalate, and the com-

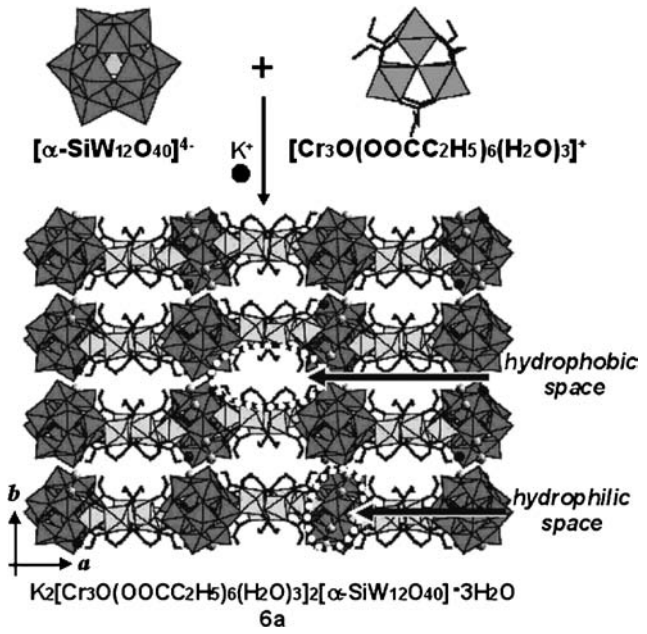

Figure 6. Synthesis and crystal structure of **6a**. Dark gray and light gray polyhedra in the polyoxometalates are $[WO_6]$ and $[SiO_4]$ units, respectively. Light gray polyhedra in the macrocation are $[CrO_6]$ units. Black and white spheres are K^+ and oxygen atom of the water of crystallization, respectively.

pound with the smaller anion charge included larger alcohols. The difference in the alcohol sorption among **3b**–**5b** is explained by the differences in the void sizes, which decreased with the increase in the anion charges.

♦ Construction of Both Hydrophilic and Hydrophobic Spaces

The ionic crystals **1a**–**5a**/**1b**–**5b** with the macrocation of $[Cr_3O(OOCH)_6(H_2O)_3]^+$ possessed only hydrophilic channels in the crystal lattice. Therefore, the complexation of macrocation of $[Cr_3O(OOCC_2H_5)_6(H_2O)_3]^+$ with the Keggin-type $[\alpha\text{-}SiW_{12}O_{40}]^{4-}$ polyoxometalate was attempted.

Figure 6 shows the schematic illustration of the synthesis and crystal structure of $K_2[Cr_3O(OOCC_2H_5)_6(H_2O)_3]_2[\alpha\text{-}SiW_{12}O_{40}]\cdot 3H_2O$ [**6a**]. The compound **6a** was composed of layers running along the *ac* plane and the spacing between the layers was 9.7 Å. In the layers, the distances between the oxygen atoms of the polyoxometalates and macrocations, those of the adjacent macrocations, and those of the water of crystallization and macrocation were 2.6–3.1 Å and within hydrogen-bonding distances. These multiple hydrogen bondings as well as Coulomb interactions were observed in the *ac* plane, probably stabilizing of the layer. As indicated by the broken line in Figure 6, straight channels ran along the *a* axis between the two layers and no water of crystallization was found. The channel was surrounded by propionate ligands of the macrocations. The opening of the channel was ca. 2.5 × 5.1 Å.

On the other hand, winding hydrogen-bond networks of the water of crystallization existed along the [110] direction through the layers. The narrowest and widest openings of the hydrophilic network channel were ca. 2.5 and 4.3 Å, respectively. The 3 mol mol^{-1} of the water of crystallization in **6a** existed in two sites O1 and O2 with occupancies of 1 and 0.5, respectively, and was in the vicinity of the potassium ions (K^+–O1 = 3.1 Å, K^+–O2 = 2.5 Å). Thus, the compound **6a** has both hydrophilic and hydrophobic channels in the crystal lattice, which is different from the fact that **1a** has only the hydrophilic channel. The straight channel surrounded by the propionate ligands of the macrocation is designated as hydrophobic channel, and the winding channel containing the water of crystallization is designated as the hydrophilic channel.

The water of crystallization in **6a** was completely desorbed by the evacuation at room temperature to form guest free phase **6b**. Single-crystal structure analyses of **6b** showed that the crystal structure was essentially the same with **6a**. Figure 3C summarizes the amounts of sorption for **6b**. The sorption isotherms showed that compound **6b** sorbs various kinds of polar organic molecules and the amounts of ≤C3 alcohols were comparable to or larger than that of water, while chlorocarbons without hydrogen-bonding ability and nonpolar molecules were excluded. Thus, **6b** showed the amphiphilic sorption property. The states of the polar organic molecules sorbed in **6b** have been quantitatively investigated using ethanol as a probe molecule. The IR and NMR studies combined with the sorption kinetics reveal that ethanol molecules are mainly sorbed into the hydrophilic channel at $P/P_0 \leq 0.5$, while the sorption into the hydrophobic channel is dominant at $P/P_0 > 0.5$. Thus, it is demonstrated that ethanol molecules enter both hydrophilic and hydrophobic channels of **6b**.

♦ Future View

This review illustrated our recent studies on the control of the structures and sorption properties of ionic crystals of polyoxometalates with a macrocation by systematically changing charges of the polyoxometalates and the bridging ligand of the macrocation. The followings are the future goals to be achieved.

(1) **Separation of azeotropic mixtures and close-boiling mixtures:** A systematic change of the size, shape, hydrophilicity/hydrophobicity of the nanospace would control the interaction between the guest molecules and the solid hosts, leading to the highly selective guest sorption. The target separations are water/alcohol, small (≤C4) alkanes and alkenes, BTX (benzene–toluene–xylene), stereoisomers, etc.

(2) **Catalysis in the nanostructure:** Polyoxometalates catalyze oxidation or acid–base reactions, and the catalytic properties can be controlled at atomic or molecular levels. For example, $[\gamma\text{-}SiW_{10}O_{34}(H_2O)_2]^{4-}$ and $[\gamma\text{-}1,2\text{-}H_2SiV_2W_{10}O_{40}]^{4-}$ can catalyze the epoxidation reactions of alkenes with high yields of epoxides and high efficiency of H_2O_2 use.[55–58] Complexation of polyoxometalates with macrocations would work as heterogeneous catalysts. Moreover, a unique reaction would proceed in the nanospace or by the cooperation with the macrocation.

This work was supported in part by the Core Research for Evolutional Science and Technology (CREST) program of the Japan Science and Technology Agency (JST) and Grant-in-Aid for Scientific Research from the Ministry of Education, Culture, Sports, Science and Technology of Japan.

References

1 M. E. Davis, *Nature* **1992**, *417*, 813.
2 A. Corma, F. Rey, S. Valencia, J. L. Jorda, J. A. Rius, *Nat. Mater.* **2003**, *2*, 493.
3 S. M. Kuznicki, V. A. Bell, H. W. Hillhouse, R. M. Jacubinas, C. M. Braunbarth, B. H. Toby, M. Tsapatsis, *Nature* **2001**, *412*, 720.
4 P. B. Weisz, V. J. Frilette, *J. Phys. Chem.* **1960**, *64*, 382.
5 M. J. Zaworotko, B. Moulton, *Chem. Rev.* **2001**, *101*, 1629.
6 G. Férey, *Chem. Mater.* **2001**, *13*, 3084.
7 M. E. Kosal, J. H. Chou, S. R. Wilson, K. S. Suslick, *Nat. Mater.* **2002**, *1*, 118.
8 S. Kitagawa, R. Kitaura, S. Noro, *Angew. Chem., Int. Ed.* **2004**, *43*, 2334.
9 H. L. Ngo, W. Lin, *Top. Catal.* **2005**, *34*, 85.
10 G. Férey, C. Mellot-Draznieks, C. Serre, F. Millange, J. Dutour, S. Surblé, I. Margiolaki, *Science* **2005**, *309*, 2040.
11 O. Ohmori, M. Kawano, M. Fujita, *Angew. Chem., Int. Ed.* **2005**, *44*, 1962.
12 M. Eddaudi, J. Kim, N. Rosi, D. Vodak, J. Wachter, M. O'Keefee, O. M. Yaghi, *Science* **2002**, *295*, 469.
13 D. N. Dybtsev, H. Chun, S. H. Yoon, D. Kim, K. Kim, *J. Am. Chem. Soc.* **2004**, *126*, 32.
14 L. Pan, K. M. Adams, H. E. Hernandez, X. Wang, C. Zheng, Y, Hattori, K. Kaneko, *J. Am. Chem. Soc.* **2003**, *125*, 3062.
15 V. S. Nayak, J. B. Moffat, *J. Phys. Chem.* **1988**, *92*, 7097.
16 A. J. Flectcher, E. J. Cussen, D. Bradshaw, M. J. Rosseinsky, K. M. Thomas, *J. Am. Chem. Soc.* **2004**, *126*, 9750.
17 M. P. Suh, J. W. Ko, H. J. Choi, *J. Am. Chem. Soc.* **2002**, *124*, 10976.
18 M. H. Zeng, X. L. Feng, X. M. Chen, *Dalton Trans.* **2004**, 2217.
19 J. Padin, S. U. Rege, R. T. Yang, L. S. Cheng, *Chem. Eng. Sci.* **2000**, *55*, 4525.
20 S. Nair, Z. Lai, V. Nikolakis, G. Xomeritakis, G. Bonilla, M. Tsapatsis, *Microporous Mesoporous Mater.* **2001**, *48*, 219.
21 F. Cavani, F. Trifiro, A. Vaccari, *Catal. Today* **1991**, *11*, 173.
22 Special issue on pillared clays, ed. by R. Burch, *Catal. Today* **1988**, *2*, 185.
23 S. J. Gregg, K. S. W. Sing, *Adsorption, Surface Area and Porosity*, Academic Press, London, **1982**, p. 237.
24 R. W. Mooney, A. G. Keenan, L. A. Wood, *J. Am. Chem. Soc.* **1952**, *74*, 1367.
25 R. M. Barrer, D. M. MacLeod, *Trans. Faraday Soc.* **1954**, *50*, 980.
26 S. Yamanaka, F. Kanamaru, M. Koizumi, *J. Phys. Chem.* **1974**, *78*, 42.
27 H. Cölfen, M. Antonietti, *Angew. Chem., Int. Ed.* **2005**, *44*, 5576.
28 S. Piana, M. Reyhani, J. D. Gale, *Nature* **2005**, *438*, 70.
29 T. P. Melia, W. P. Moffitt, *J. Colloid Sci.* **1964**, *19*, 433.
30 B. Judat, M. Kind, *J. Colloid Interface Sci.* **2004**, *269*, 341.
31 M. Hölscher, U. Englert, B. Zibrowius, W. F. Hölderich, *Angew. Chem., Int. Ed. Engl.* **1994**, *33*, 2491.
32 Y. Hayashi, F. Müller, Y. Lin, S. M. Miller, O. P. Anderson, R. G. Finke, *J. Am. Chem. Soc.* **1997**, *119*, 11401.
33 A. Dolbecq, C. Mellot-Draznieks, P. Mialane, J. Marrot, G. Férey, F. Sécheresse, *Eur. J. Inorg. Chem.* **2005**, 3009.
34 M. I. Khan, E. Yohannes, D. Powell, *Inorg. Chem.* **1999**, *38*, 212.
35 D. Hagrman, P. J. Hagrman, J. Zubieta, *Angew. Chem., Int. Ed.* **1999**, *38*, 3165.
36 J. H. Son, H. Choi, Y. U. Kwon, *J. Am. Chem. Soc.* **2000**, *122*, 7432.
37 W. Schmitt, E. Baissa, A. Mandel, C. E. Anson, A. K. Powell, *Angew. Chem., Int. Ed.* **2001**, *40*, 3577.
38 Y. Ishii, Y. Takenaka, K. Konishi, *Angew. Chem., Int. Ed.* **2004**, *43*, 2702.
39 M. V. Vasylyev, R. Neumann, *J. Am. Chem. Soc.* **2004**, *126*, 884.
40 M. S. Sankar, U. Kortz, *Angew. Chem., Int. Ed.* **2005**, *44*, 3777.
41 R. Atencio, A. Briceno, X. Galindo, *Chem. Commun.* **2005**, 637.
42 H. Y. An, E. B. Wang, D. R. Xiao, Y. G. Li, Z. M. Su, L. Xu, *Angew. Chem., Int. Ed.* **2006**, *45*, 904.
43 M. T. Pope, A. Müller, *Angew. Chem., Int. Ed.* **1991**, *30*, 34.
44 T. Okuhara, N. Mizuno, M. Misono, *Adv. Catal.* **1996**, *41*, 113.
45 N. Mizuno, K. Kamata, K. Yamaguchi, in *Surface and Nanomolecular Catalysis*, ed. by R. M. Richards, Taylor and Francis Group, LLC, New York, **2006**, p. 463.
46 C. L. Hill, *Chem. Rev.* **1998**, *98*, 1.
47 R. Neumann, in *Modern Oxidation Methods*, ed. by J. E. Bäckvall, Wiley-VCH, Weinheim, **2004**, p. 223.
48 C. L. Hill, in *Comprehensive Coordination Chemistry II*, ed. by J. A. McClerverty, T. J. Meyer, Elsevier, Amsterdam, **2003**, p. 679.
49 I. V. Kozhevnikov, *Catalysis by Polyoxometalates*, Wiley, Chichester, UK, **2002**.
50 S. Uchida, M. Hashimoto, N. Mizuno, *Angew. Chem., Int. Ed.* **2002**, *41*, 2814.
51 S. Uchida, N. Mizuno, *Chem. Eur. J.* **2003**, *9*, 5850.
52 S. Uchida, N. Mizuno, *J. Am. Chem. Soc.* **2004**, *126*, 1602.
53 S. Uchida, R. Kawamoto, T. Akatsuka, S. Hikichi, N. Mizuno, *Chem. Mater.* **2005**, *17*, 1367.
54 R. Kawamoto, S. Uchida, N. Mizuno, *J. Am. Chem. Soc.* **2005**, *127*, 10560.
55 N. Mizuno, K. Yamaguchi, *Chem. Rec.* **2006**, *6*, 12.
56 N. Mizuno, K. Yamaguchi, K. Kamata, *Coord. Chem. Rev.* **2005**, *249*, 1944.
57 K. Kamata, K. Yonehara, Y. Sumida, K. Yamaguchi, S. Hikichi, N. Mizuno, *Science* **2003**, *300*, 964.
58 Y. Nakagawa, K. Kamata, M. Kotani, K. Ymaguchi, N. Mizuno, *Angew. Chem., Int. Ed.* **2005**, *44*, 5136.